

## **PRACTICAL MODEL OF CRACK AND BOND SLIP FOR THERMAL CRACK ANALYSIS**

H. Morimoto and W. Koyanagi  
Department of Civil Engineering, Gifu University, Gifu, Japan

### **Abstract**

This paper deals with a practical 3-D analysis model for thermal stress and crack width. The model applied in this study is based on the concept of discrete crack approach. The authors analyzed the thermal stress and crack width in a wall structure by FEM incorporating the 3-D analysis model, and elucidated the 3-D distribution of thermal stress and crack width in the wall in comparison with the actual measurements. The effect of reinforcement on crack control was also investigated.

*Keywords: thermal crack, discrete crack model, bond slip model, 3-D FEM, crack control*

### **1. Introduction**

Cracks due to thermal stress caused by heat of hydration frequently arise in massive concrete structures. It is very important to control the crack width in the stage of design and construction, as it adversely affects the durability, functionality and esthetics of structure. The most applicable analysis method for cracked concrete member is the finite element method (FEM) with the discrete crack model and the smeared crack

model. The Japan Concrete Institute Committee on Thermal Stress of Massive Concrete Structures (JCI Mass Concrete Committee) had proposed a FEM thermal crack analysis model in 1992. However, most of the thermal crack analysis reported so far model crack two-dimensionally, even though actual cracks are considered to develop three-dimensionally. In this study, the authors analyzed the thermal stress and crack width in a wall structure by 3-D FEM incorporating a practical crack analysis model, and elucidated the 3-D distribution of thermal stress and crack width in the wall in comparison with the measurements. The investigation also covered crack width controlling effect of reinforcement.

## 2. 3-D analysis model

The 3-D analysis model applied in this study is based on the concept of the JCI Mass Concrete Committee model (JCI Committee 1992) using the discrete crack approach. As shown in Fig.1, this model expresses a crack as a gap between two nodes defined at the position of cracking. In this study, two nodes are defined at the point (double nodes) where a crack is expected to occur. Double nodes are combined with joint elements with a high rigidity until the onset of cracking. At the crack onset, the rigidity of the joint elements is minimized to express the occurrence of cracking. The concept of the bond model is shown in Fig. 2. In this model, as shown in the figure, the bond condition that continuously changes over a certain length from the crack is approximated by two zone, that is, a debonded zone and a fully bonded zone. The strain of a bar assumed to be distributed in the form of a rectangle as shown in Fig. 3. A half of the length assumed to be debonded is defined as an equivalent debonding zone,  $ls$ .

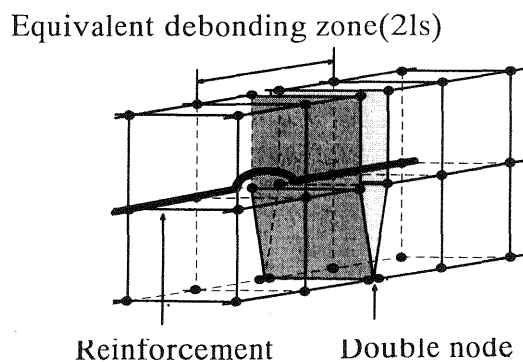


Fig. 1. 3-D analysis model

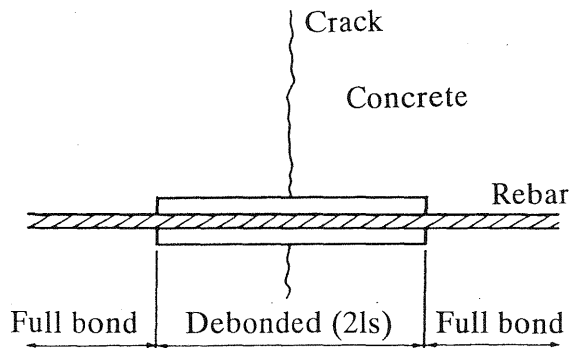


Fig. 2. Bond concept

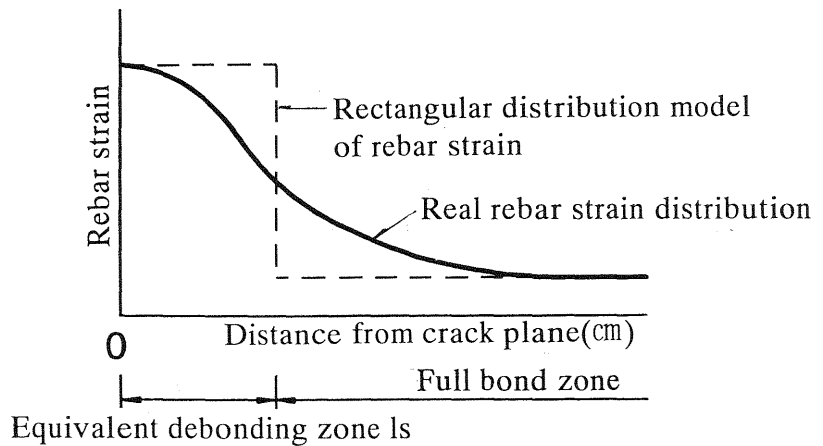


Fig. 3. Modelling of rebar strain distribution

Since the equivalent debonding zone,  $l_s$ , has a profound effect on the result of crack width analysis, appropriate zoning is of paramount importance in putting this model to practical use.

### 3. Outline of analysis

#### 3.1 Structure under analysis

The structure under analysis (JCI Committee 1986) is a wall of 1.0 m in

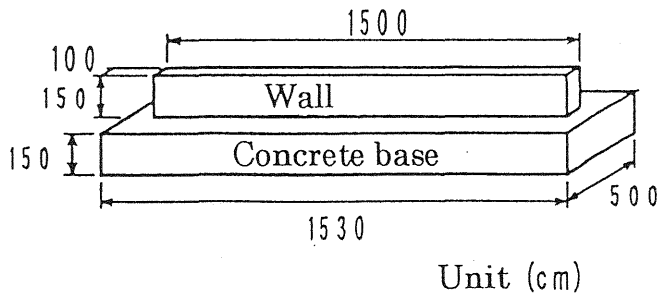


Fig. 4. Structure under analysis

width, 1.5 m in height, and 15 m in length; on a concrete base of 5.0 m in width, 1.5 m in height, and 15.3 m in length as shown in Fig. 4. D19 distributing bars are placed longitudinally at a reinforcement ratio of 0.27%. The wall is fitted with effective concrete stress gauges, reinforcement strain gauges, crack gauges, thermocouples, and stress-free strain gauges at different points, to measure the concrete stress, reinforcement stress, crack width, temperature, and thermal expansion coefficient. It should be noted that a crack across the height of the wall occurred near mid-length at the age of 7 days.

### 3.2 Analysis method

The elements were meshed so as to coincide with the distributing bars, as the reinforcing bars were modeled by bar elements. The bond with the concrete base at the bottom of the wall was assumed to be perfect so that no separation occurred even after cracking. The tensile strength,  $f_t$  ( $\text{N}/\text{mm}^2$ ), and elastic modulus,  $E$  ( $\text{KN}/\text{mm}^2$ ), were evaluated by the following equations calculated from the measurements.

$$f_t(t) = \frac{t}{1.408 + 3.43 \times 10^{-1}t} \quad (1)$$

$$E(t) = \frac{t}{1.137 \times 10^{-1} + 2.914 \times 10^{-2}t} \quad (2)$$

where  $t$  = age (days)

The occurrence of a crack was assumed when the thermal stress exceeded 80% of the tensile strength, in consideration of the rate of increase in the

thermal stress, fluctuation of strength of actual structures, and existing study results (Karino et al. 1995). The temperature of the wall section analyzed by the 2-D FEM. In the 3-D crack analysis, the temperature changes longitudinally were approximately neglected, and the 2-D temperature analysis results of the wall section was applied.

### **3.3 Items of investigation**

(1) Effects of equivalent debonding zone,  $l_s$ , on the calculation results  
The selection of an appropriate equivalent debonding zone to express bond slip is critical in the analysis model shown in Fig. 1. Accordingly, the authors investigated the effects of  $l_s$  on the calculation results, as well as appropriate values for  $l_s$ . Analysis was carried out for four values of  $l_s$ ; 5, 10, 15, and 20 cm.

(2) 3-D distribution of thermal crack width in the wall  
Thermal crack width is considered to change in both directions of the wall height and thickness. The authors therefore investigated the 3-D distribution of thermal crack width and thermal stresses in the wall by 3-D analysis. Accuracy of the 3-D analyses was then verified by comparison with the actual measurements.

(3) Crack width controlling effect of reinforcement  
Placing the so-called "crack controlling bars", or bars perpendicular to cracks, is effective as a means of controlling the crack width[4]. In this study, to elucidate the relationship between the reinforcement content and the crack width reinforcement ratios of 0.27%, 0.6%, and 0.9% were adopted for the 3-D analyses.

## **4. Analysis results**

### **4.1 Effect of equivalent debonding zone**

#### **(1) Crack width**

Figures 5 to 7 show the measured crack width on the surface at the mid-height of the wall, as well as the calculated values, with the  $l_s$  values being 10, 15, and 20 cm. The measured crack width immediately after the occurrence was around 0.27 mm. Crack width tended to increase slightly with an increase in age, reaching 0.37 mm at 14 days. According to the analysis, cracking occurred at 5 days in all cases, and the crack width tended to increase slightly thereafter, similar to actual measurements. The larger crack width at mid-thickness compared to that near the surface is due to a higher tensile stress occurring at mid-thickness. As  $l_s$  expresses the bond slip, a large  $l_s$  means that a large bond slip zone is assumed. The figures show that a large value of  $l_s$  leads to a large crack width by calculation. This indicates that a larger bond slip zone leads to a larger crack width. When comparing the calculated and measured crack widths

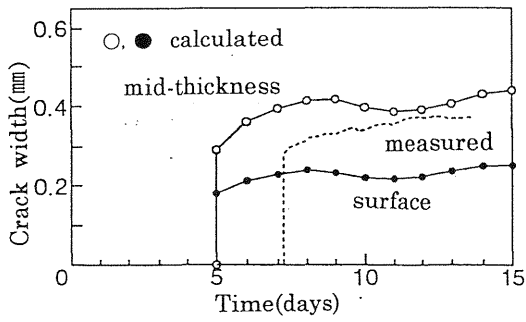


Fig. 5. Development of crack width( $l_s=10$  cm)  
(Mid-height level of the wall)

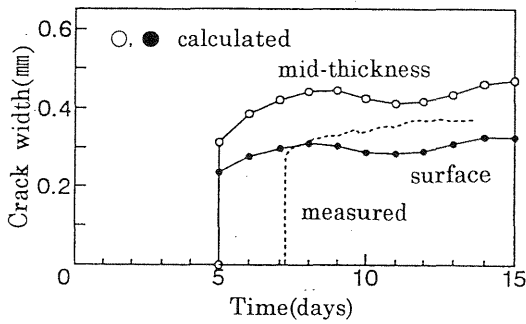


Fig. 6. Development of crack width( $l_s=15$  cm)  
(Mid-height level of the wall)

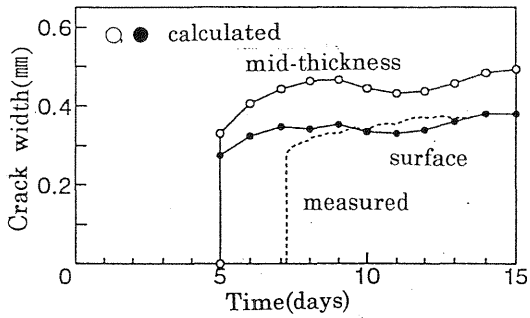


Fig. 7. Development of crack width( $l_s=20$  cm)  
(Mid-height of the wall)

on the surfaces at the wall's mid-height in Figures 5 to 7, with  $l_s$  being 15 cm and 20 cm, the calculated maximum crack widths agree well with the measured value of 0.37 mm. Consequently, 15 to 20 cm are considered to be appropriate  $l_s$  values for the 3-D analysis models.

(2) Reinforcement stress

The calculated reinforcement stress decreases as the  $l_s$  value increases. This is because a larger value of  $l_s$  leads to a lower average strain of reinforcement in the equivalent debonding zone. Figure 8 shows the measured reinforcement stress at the wall's mid-height crack position and calculated reinforcement stress for the  $l_s$  value being 15 cm. The figures indicate a tendency of reinforcement stress history similar to that of crack width. The measured reinforcement stress at 8 days is approximately  $210 \text{ N/mm}^2$ . The calculated reinforcement stress with  $l_s$  being 15 cm is approximately  $215 \text{ N/mm}^2$ , agreeing well with the actual measurements. The calculated values with  $l_s$  at 20 cm also agrees well with actual measurements. Accordingly, the  $l_s$  values of 15 to 20 cm are also found to lead to good calculation results in regard to reinforcement stress.

(3) Concrete stress

Figure 9 shows the measured concrete stress at a section of the wall's mid-height approximately 2 m away from the crack and the corresponding values calculated with  $l_s$  being 15 cm. The calculated values at mid-thickness and on the surface are shown. From the figure, calculated stress slightly exceeds the measured stress in regard to compressive stress at early ages. However, calculated and measured stress agree well regarding the tensile stress that gradually develops with a drop in wall temperature. Stress released due to cracking is observed in the calculated surface stress at 5 days. No marked effect of  $l_s$  on the concrete stress was observed.

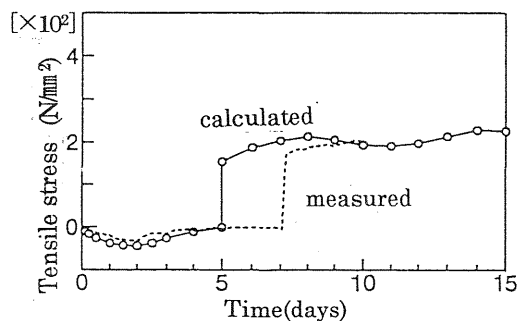


Fig. 8. Development of reinforcement stress ( $l_s=15 \text{ cm}$ )

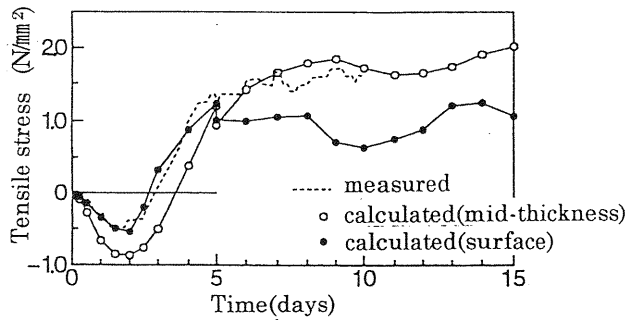


Fig. 9. Development of concrete stress ( $l_s=15$  cm)

#### 4.2 3-D distribution of thermal stress and crack width

Figure 10 displays the 3-D distribution of concrete stress of a section at approximately 2 m from the crack with  $l_s$  being 15 cm. The distribution contour of the section, resulting from the combined internal and externally restrained stresses, changes from concave to convex with an increase in age. Figure 11 shows the crack width with  $l_s$  being 15 cm. The crack width distribution is expressed as a contour convex towards upper center having its peak at mid-thickness near the top of the wall. In other words, the crack width in the center is larger than that on the surface. The contour of crack width distribution remains unchanged over time.

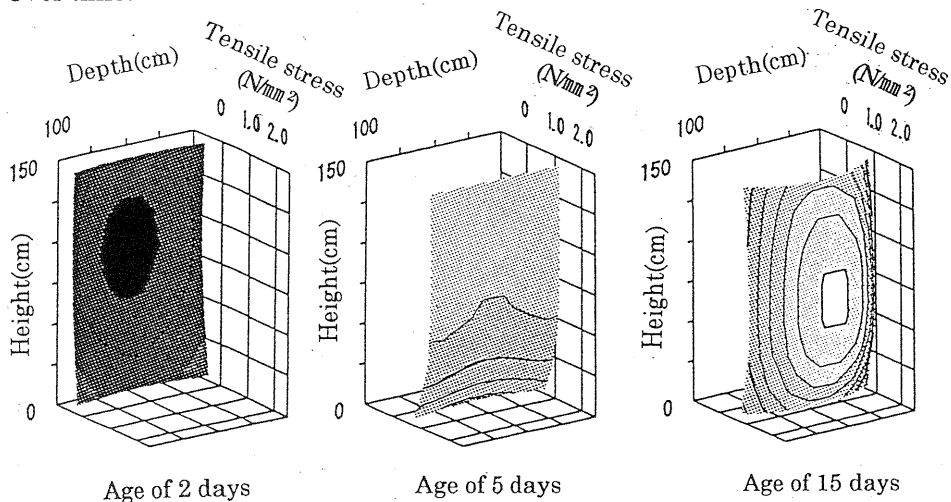


Fig. 10. 3-D distribution of concrete stress in the wall

#### 4.3 Crack width controlling effect of reinforcement

Figure 12 shows 3-D distribution of the crack width at 9 days with the



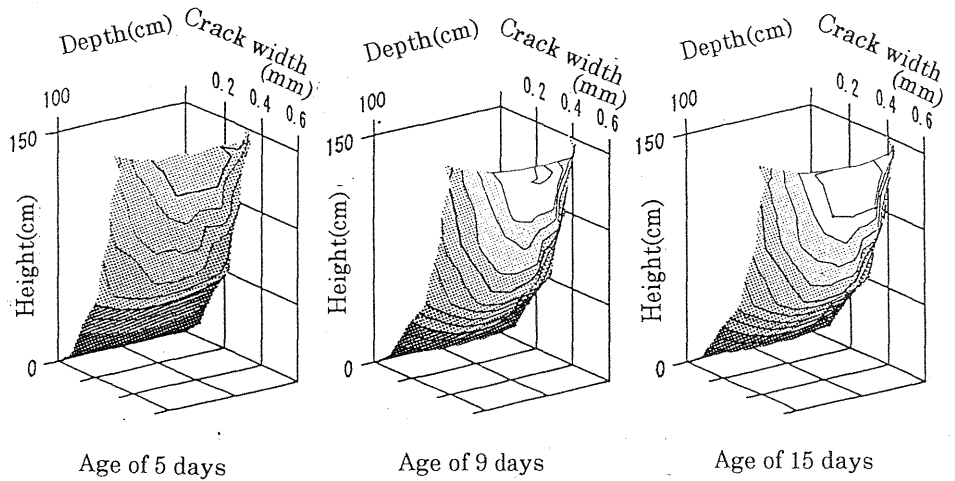


Fig. 11. 3-D distribution of crack width in the wall

reinforcement ratio being 0.27%, 0.6%, and 0.9%. The figure reveals that crack width is reduced over the entire section with an increase in reinforcement. No marked change is observed between the contours of crack width distribution with different reinforcement ratios. The maximum crack width is reduced to 58% and 40% when the reinforcement ratio is increased to 0.6% and 0.9%, respectively, when compared with the reinforcement ratio of 0.27%. In other words, according to the results of this analysis, the maximum crack width is

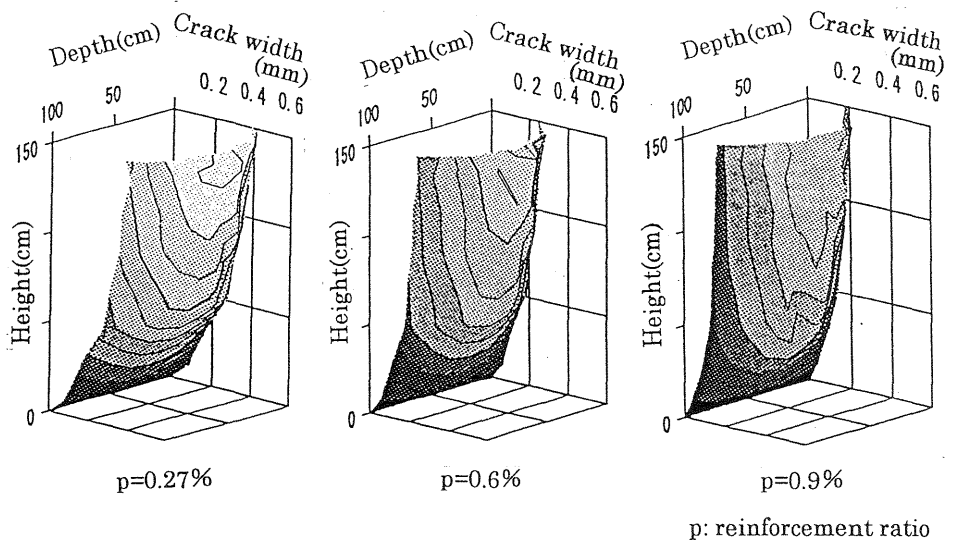


Fig. 12. Crack width controlling effect of reinforcement

0.47mm when the distributing bar ratio is 0.27%, which is normal practice; but the maximum crack width can be limited to under 0.2 mm, which is generally a standard of allowable crack width, by placing distributing bars at a reinforcement ratio of 0.6% or more.

## 5. Conclusions

In this study, the authors elucidated the 3-D distribution of thermal stress and crack width using the FEM into which a 3-D crack analysis model is incorporated. The investigation covered the optimum characteristic value,  $l_s$ , of the analysis model and the crack width controlling effect of reinforcement. The results obtained in this study are summarized as follows:

- (1) Thermal crack width, concrete stress, and reinforcement stress can be estimated accurately by using a 3-D crack width analysis model. The characteristic value of the analysis model,  $l_s$ , strongly affects the calculations of crack width and reinforcement stress. The optimum characteristic  $l_s$  value is 15 to 20 cm.
- (2) The distribution of thermal crack width in the wall forms a contour convex towards the upper center having the peak at mid-thickness near the top of the wall. The distribution contour remains unchanged with time. The  $l_s$  value has no effect on the contour. The contour of concrete stress distribution changes from concave to convex with time.
- (3) An adequate amount of reinforcement effectively controls the crack width. As the reinforcement content increases, the crack width is reduced over the entire wall section.

## 6. References

- JCI committee on Thermal Stress of Massive Concrete Structure (1992)  
A Proposal of a Method of Calculating Crack Width Due to Thermal Stress, **JCI Committee Report**.
- JCI Committee for Research and Study on Concrete Cracking (1986)  
Recommendation for Control of Cracking in Massive Concrete, **JCI Committee Report**. (in Japanese)
- Karino, T., Watanabe, H. and Khono, H. (1995) Tensile Strength Characteristics of Concrete for Evaluation of Thermal Cracking, **Annual Meeting of JSCE**, 50, 5, 732-733. (in Japanese)
- JSCE (1996) **Standard Specification for Design and Construction for Concrete Structures (Part II Construction)**.